

Gene therapy supports long-term reconstitution of patient hematopoietic stem cells in deficiency of adenosine deaminase 2

Chiara Rigamonti,^{1,2} Dimitri Bulté,¹ Federica Barzaghi,^{1,3} Cristina Mesa-Núñez,¹ Luca Basso-Ricci,¹ Emanuela Pettinato,¹ Camilla Visconti,^{2,3} Sara Degl'Innocenti,⁴ Francesco Gazzo,^{1,6} Fabrizio Benedicenti,¹ Sergio Arévalo,¹ Pamela Quaranta,¹ Francesca Sanvito,^{4,5} Roberta Caorsi,⁷ Francesca Schena,⁷ Michela Lupia,⁸ Silvia Federici,⁹ Antonella Insalaco,⁹ Fabrizio De Benedetti,⁹ Serena Scala,¹ Maurizio Miano,⁸ Francesca Conti,^{10,11} Maria Pia Cicalese,^{1,2,3} Eugenio Montini,¹ Marco Gattorno,⁷ Carlo Dufour,⁸ Alessandro Aiuti,^{1,2,3} and Alessandra Mortellaro¹

¹San Raffaele Telethon Institute for Gene Therapy (SR-Tiget), IRCCS San Raffaele Scientific Institute, 20132 Milan, Italy; ²Vita-Salute San Raffaele University, 20132 Milan, Italy; ³Pediatric Immunohematology and Bone Marrow Transplantation Unit, IRCCS San Raffaele Scientific Institute, 20132 Milan, Italy; ⁴GLP Test Facility, San Raffaele Telethon Institute for Gene Therapy (SR-Tiget), IRCCS San Raffaele Scientific Institute, 20132 Milan, Italy; ⁵Pathology Unit, IRCCS San Raffaele Scientific Institute, 20132 Milan, Italy; ⁶Department of Electronics, Information and Bioengineering, Politecnico di Milano, 20133 Milan, Italy; ⁷UOC Rheumatology and Autoinflammatory Diseases, IRCCS Istituto Giannina Gaslini, 16147 Genoa, Italy; ⁸Hematology Unit, IRCCS Istituto Giannina Gaslini, 16147 Genoa, Italy; ⁹Division of Rheumatology, Bambino Gesù Children's Hospital, ERN-RITA Center, IRCCS, 00165 Rome, Italy; ¹⁰Pediatric Unit, IRCCS Azienda Ospedaliero-Universitaria di Bologna, 40138 Bologna, Italy; ¹¹Department of Medical and Surgical Sciences, Alma Mater Studiorum, University of Bologna, 40126 Bologna, Italy

Deficiency of adenosine deaminase 2 (DADA2) is a monogenic autoinflammatory disorder characterized by systemic inflammation, vasculopathy, immunodeficiency, and bone marrow failure. Current therapies—including anti-TNF agents and allogeneic hematopoietic stem cell transplantation (HSCT)—have limitations, especially for patients with hematologic involvement or no matched donor. We developed a lentiviral vector (LV.ADA2) to restore ADA2 expression in patient hematopoietic stem and progenitor cells (HSPCs) and evaluated its safety and efficacy in preclinical models. LV.ADA2 transduction of mobilized peripheral blood HSPCs from healthy donors resulted in stable ADA2 expression and secretion without impairing clonogenicity, multilineage differentiation, or long-term engraftment in immunodeficient mice. In HSPCs from 12 DADA2 patients, LV.ADA2 restored ADA2 protein and enzymatic activity preserving colony-forming ability and multilineage differentiation *in vitro*. *In vivo*, gene-corrected patient-derived HSPCs sustained long-term engraftment and multilineage reconstitution comparable to healthy controls. Integration site analysis confirmed a polyclonal pattern of hematopoietic reconstitution across all experimental settings, with no evidence of clonal dominance. Together, these findings demonstrate that ADA2 gene therapy with a LV is safe, maintains HSPC functionality, and enables durable hematopoietic reconstitution in a mouse model, providing a strong foundation for clinical translation and as a curative alternative to allogeneic HSCT in DADA2.

INTRODUCTION

Deficiency of adenosine deaminase 2 (DADA2) is a recently identified autosomal recessive disorder of the immune system caused by biallelic mutations in the *ADA2* gene, which encodes the secreted enzyme adenosine deaminase 2.^{1,2} This enzyme catalyzes the deamination of adenosine to inosine and is predominantly produced by myeloid cells, particularly monocytes and macrophages.³

Clinically, DADA2 presents with a broad spectrum of manifestations, including systemic inflammation, vasculitis/vasculopathy resembling polyarteritis nodosa with early-onset strokes, mild immunodeficiency characterized by hypogammaglobulinemia and low switched memory B cells, and most critically, hematological abnormalities.^{4,5} These hematologic complications range from isolated cytopenia to severe bone marrow failure (BMF), including anemia, lymphopenia, neutropenia, and thrombocytopenia.^{5,6} We recently reported that bone marrow (BM) abnormalities in DADA2 may arise early and silently, even in the absence of overt hematologic symptoms.⁷

Diagnosis relies on the detection of absent or significantly reduced ADA2 enzymatic activity in plasma, followed by confirmation of

Received 16 September 2025; accepted 28 October 2025;
<https://doi.org/10.1016/j.omtm.2025.101624>

Correspondence: Alessandra Mortellaro, San Raffaele Telethon Institute for Gene Therapy (SR-Tiget), IRCCS San Raffaele Scientific Institute, Via Olgettina 60, 20132 Milan, Italy.

E-mail: mortellaro.alessandra@hsr.it



pathogenic variants in ADA2.⁸ If left untreated or undiagnosed, DADA2 can lead to life-threatening complications, with an estimated lethality of 8% and a mean survival age of 35 years.⁹

Currently, there are no targeted therapies for DADA2. Anti-TNF agents are the standard of care and can effectively reduce systemic inflammation, control vasculitis, and prevent strokes.^{6,8,10} Allogeneic hematopoietic stem cell transplantation (HSCT) offers a curative option, successfully restoring enzymatic activity and correcting the hematologic, immunologic, and inflammatory features of the disease.^{11–16} However, HSCT carries substantial risks, particularly in patients lacking a suitable donor, and may be complicated by graft-versus-host disease, infections, transplant rejection, and the need for long-term immunosuppression.

Given the significant unmet clinical need, alternative therapeutic strategies are urgently required. *Ex vivo* gene therapy offers a promising curative approach for monogenic immune-mediated disorders.¹⁷ Lentiviral (LV) gene addition into autologous hematopoietic stem and progenitor cells (HSPCs) enables stable integration and sustained expression of the therapeutic gene, providing a lifelong source of corrected immune and hematopoietic cells. Compared to allogeneic HSCT, gene therapy offers the key advantage of using the patient's own cells, thereby eliminating the risks of graft-versus-host disease, transplant rejection, and the challenges associated with donor availability and HLA matching. Moreover, the use of autologous cells allows for reduced-intensity conditioning regimens, which is particularly beneficial for patients with severe disease manifestations who may not tolerate myeloablative conditioning.

Recent studies, including our own, have demonstrated the feasibility of HSPC gene therapy for DADA2 using LVs encoding ADA2.^{3,18} Reconstitution of ADA2 expression in patient-derived monocytes or HSPC-derived macrophages led to a marked reduction in inflammatory cytokine release, including TNF, IL-6, and IFN. However, the long-term impact of ADA2 correction on the *in vivo* fitness and multipotency of patient-derived HSPCs remains unexplored.

In this study, we show the feasibility and therapeutic potential of LV-mediated gene transfer in HSPCs derived from a cohort of patients with DADA2 using the self-inactivating LV.ADA2. ADA2 restoration in patients' HSPCs enables long-term hematopoietic reconstitution without affecting clonogenicity, differentiation, or safety, supporting its therapeutic potential. Integration site analysis confirmed polyclonal reconstitution without insertional bias.

RESULTS

LV.ADA2-mediated ADA2 overexpression is well tolerated and preserves the functional properties of healthy donor-derived CD34⁺ cells

To assess the impact of ADA2 overexpression on HSPCs, CD34⁺ cells isolated from mobilized peripheral blood (mPB) of three healthy donors (HDs) were transduced with either the therapeutic LV.ADA2 or the control LV.GFP³ (Figure 1A) at multiplicities of

infection (MOIs) of 25 and 50, both within clinically relevant ranges. Fourteen days post-transduction, droplet digital PCR revealed a dose-dependent increase in the frequency of vector-positive granulocyte-macrophage (CFU-GM) and burst-forming unit-erythroid (BFU-E) colonies, with levels comparable between LV.ADA2 and LV.GFP (Figure 1B). The average LV.ADA2 vector copy number (VCN) per genome in CFU-GM colonies was 1.42 ± 1.51 and 3.54 ± 3.49 at MOI 25 and 50, respectively. In BFU-E colonies, LV.ADA2 VCNs were 1.33 ± 0.875 at MOI 25 and 5.83 ± 5.53 at MOI 50, confirming efficient gene delivery (Figure 1C). ADA2 overexpression was confirmed by western blot in myeloid cultures derived from transduced and untransduced CD34⁺ cells, with robust secretion of ADA2 protein into the culture supernatant at MOI 50 (Figure 1D). Enzymatic activity assay confirmed increased ADA2 activity in the culture supernatants of LV.ADA2-transduced cells at MOI 50 (Figure S1).

Total cell expansion was not significantly altered by LV.ADA2 transduction compared to mock (cells cultured without the vector) or LV.GFP controls (Figure 1E). Similarly, the number and proportion of CFU-GM and BFU-E colonies remained stable (Figure 1F). Moreover, *in vitro* differentiation into the myeloid, lymphoid, erythroid, and megakaryocyte/platelet lineages was not affected by ADA2 overexpression (Figure S2).

These data indicate that ADA2 overexpression by LV transduction does not impair the proliferative or clonogenic capacity of mPB-derived HDs' CD34⁺ cells.

ADA2 overexpression does not impair *in vivo* engraftment or multilineage output of mobilized CD34⁺ cells from HDs

To evaluate the *in vivo* effects of LV ADA2 overexpression, CD34⁺ cells isolated from mPB of three HDs were either mock-transduced or transduced with LV.GFP or LV.ADA2 at MOIs of 25 or 50, and subsequently transplanted into NSGW41 immunodeficient mice. Hematopoietic reconstitution was monitored over 18 weeks. All transplanted mice showed steady body weight gain throughout the observation period, indicating no overt toxicity or adverse effects due to ADA2 overexpression (Figure 2A).

At endpoint, flow cytometry analysis of BM revealed similar levels of human CD45⁺ cell engraftment across all conditions, with no significant differences in either the proportion or absolute number of cells between mock-, LV.GFP-, and LV.ADA2-transplanted groups (Figure 2B). VCN analysis demonstrated stable engraftment of transduced cells in BM, spleen, and peripheral blood up to 18 weeks following transplantation (Figure 2C). Quantification of HSPC subsets, including primitive HSCs and lineage-committed progenitors (myeloid, erythroid, lymphoid, and megakaryocytic), confirmed comparable frequencies and absolute counts across all groups (Figure 2D). Peripheral blood analysis at 18 weeks post-transplant showed consistent CD45⁺ cell frequencies among groups (Figure S3A), and multilineage hematopoietic output—including monocytes, polymorphonuclear (PMN) cells, B and T lymphocytes,

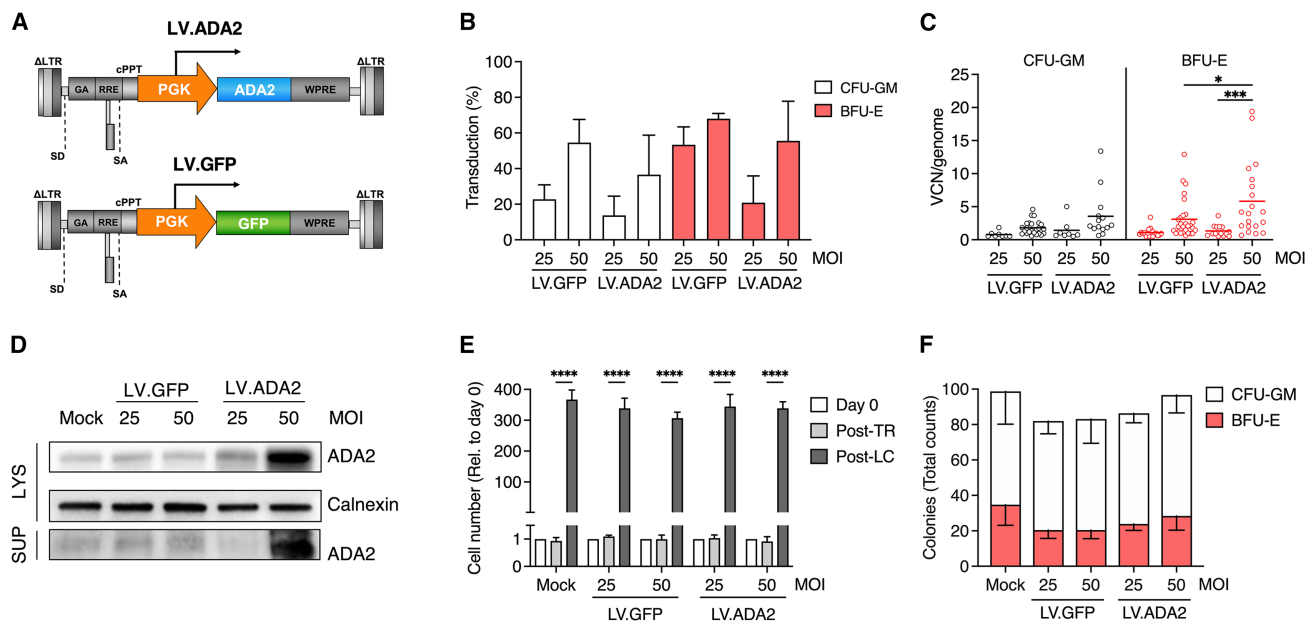


Figure 1. Lentiviral-mediated ADA2 delivery enables stable expression in HD CD34⁺ cells without impairing *in vitro* expansion and colony-forming capacity

(A) Diagram of the lentiviral vectors used in this study. (B) Transduction efficiency of LV.ADA2 and LV.GFP at MOIs 25 and 50, expressed as the percentage of vector-positive colonies (VCN \geq 0.5) among total CFUs, measured by droplet digital PCR. (C) Average vector copy number (VCN) per genome in granulocyte-macrophage (CFU-GM) and burst-forming unit-erythroid (BFU-E) colonies derived from transduced CD34⁺ cells. (D) Western blot analysis of intracellular ADA2 expression and secretion in supernatants of mock CD34⁺ cells (cells cultured without vector), or transduced with LV.ADA2 or LV.GFP, 14 days post-transduction. Calnexin was used as a loading control. (E) Fold expansion of CD34⁺ cells over 14 days in liquid culture following transduction. (F) Quantification and distribution of myeloid (CFU-GM) and erythroid (BFU-E) colonies derived from mock-, LV.GFP-, or LV.ADA2-transduced CD34⁺ cells. Bar graphs show mean \pm standard error of the mean from three independent HDs. Violin plots depict median and IQR. **, $p < 0.01$; ***, $p < 0.001$; ****, $p < 0.0001$. Lys, total cell protein extracts; Sup, cell supernatants.

and NK cells—was preserved in LV.ADA2-transplanted mice (Figure S3B).

Colony-forming assays using BM-derived CD45⁺ cells from mice revealed similar CFU-GM and BFU-E output across experimental groups, indicating preserved clonogenic potential (Figure 2E).

Macroscopic evaluation of the examined internal organs revealed no abnormalities. Histological examination of hematopoietic tissues showed no evidence of malignancy or tissue damage associated with ADA2 overexpression. Both spleen and BM sternum showed similar degree of humanization across all transplanted mice, without evidence of inflammation or proliferative changes (Figure S4).

Taken together, these findings demonstrate that LV.ADA2-mediated ADA2 overexpression is well tolerated *in vivo*, preserves HSPC function and hematopoietic differentiation, supporting the preclinical safety of this gene therapy approach in a humanized model.

LV.ADA2 restores ADA2 expression in DADA2 patients' HSPCs without impairing their clonogenic or differentiation potential

To evaluate the efficacy of LV.ADA2 in correcting the molecular defect in DADA2, BM-derived CD34⁺ cells from 12 DADA2 patients

were transduced with LV.ADA2 at a MOI of 50. Transduction efficiency, assessed by droplet digital PCR in individual CFU-GM and BFU-E colonies, exceeded 85% on average for both colony types (Figure 3A). The median VCN ranged from 6.69 ± 3.65 in CFU-GM to 8.06 ± 3.80 in BFU-E colonies, confirming robust gene transfer (Figure 3B).

Western blot analysis of CD34⁺ cells from a representative patient, expanded *in vitro* with cytokine support, showed absence of ADA2 expression in untransduced DADA2 cells, while LV.ADA2 transduction led to robust intracellular ADA2 protein expression (Figure 3C). Consistently, ADA2 enzymatic activity was markedly increased in the culture supernatants of LV.ADA2-transduced patient cells, reaching or exceeding the levels observed in mock-transduced HD cells (Figure 3D).

Assessment of clonogenic potential confirmed that colony numbers from DADA2 patient-derived CD34⁺ cells were reduced compared to HD cells cultured without the vector (mock), particularly in granulocyte-erythrocyte-monocyte-megakaryocyte (GEMM) and CFU-GM colonies.⁷ Although colony numbers from DADA2 CD34⁺ cells were lower than those typically observed in HDs, LV.ADA2 transduction did not further reduce their clonogenic potential (Figure 3E). Moreover, in a multi-lineage *in vitro* differentiation

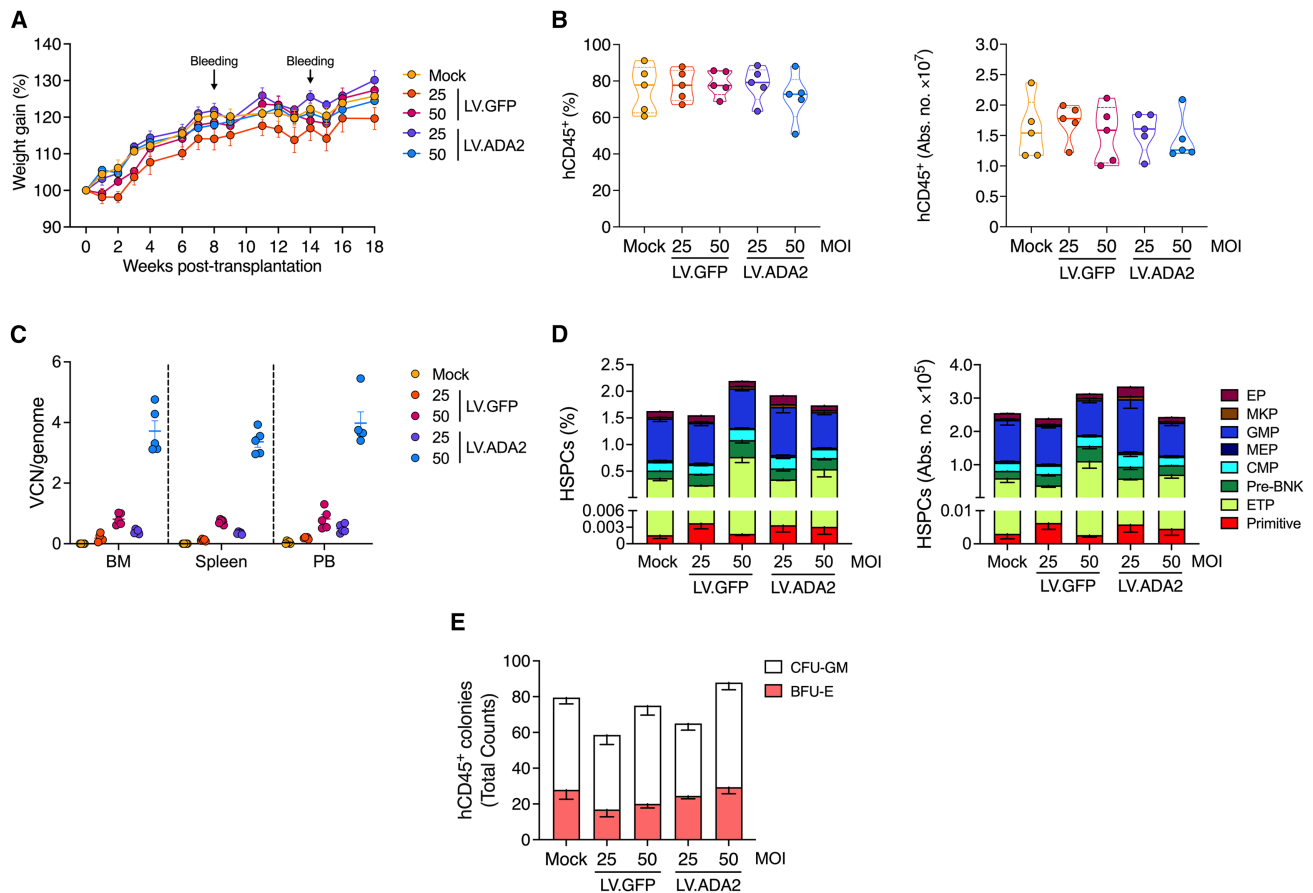


Figure 2. ADA2 overexpression via lentiviral transfer supports long-term engraftment and multilineage differentiation of HD HSPCs in NSGW41 mice without adverse effects

(A) Time course analysis of body weight following transplantation with mPB CD34⁺ cells from HDs transduced with either LV.GFP or LV.ADA2 at two multiplicities of infection (MOI 25 and 50), shown as percentage of initial weight. Arrows indicate blood sampling time points. (B) At endpoint, human chimerism was evaluated in the BM as both the percentage and absolute number of human CD45⁺ cells. (C) Vector copy number (VCN) per genome measured in total peripheral blood, bone marrow, and spleen at 18 weeks post-transplantation in NSGW41 mice receiving LV.ADA2- or LV.GFP-transduced mPB CD34⁺ cells. Data are presented as mean \pm standard error of the mean. (D) Flow cytometry was used to quantify primitive HSPCs and committed progenitor populations in the BM at endpoint, including erythroid progenitors (EP), megakaryocyte progenitors (MKP), granulocyte-monocyte progenitors (GMP), megakaryocyte-erythroid progenitors (MEP), common myeloid progenitors (CMP), precursors of B and NK cells (Pre-BNK), and early T progenitors (ETP). (E) Colony-forming unit (CFU) assays were performed on ex vivo-isolated human CD45⁺ bone marrow cells to assess myeloid (CFU-GM) and erythroid (BFU-E) progenitor output under mock- (cells cultured without vector), LV.GFP-, or LV.ADA2-transduced conditions. Data are shown as mean \pm standard error of the mean.

assay, ADA2 overexpression had no adverse effect on the generation of erythroid, myeloid, lymphoid, or megakaryocyte/platelet lineages (Figure 3F).

These results demonstrate that LV.ADA2 efficiently reconstitutes ADA2 expression and activity in patient-derived HSPCs while preserving their clonogenic capacity and multilineage differentiation potential.

ADA2 gene correction preserves the engraftment and hematopoietic reconstitution potential of patient-derived CD34⁺ cells *in vivo*

To assess the *in vivo* functionality of ADA2-corrected HSPCs, BM-derived CD34⁺ cells from DADA2 patients—either mock-trans-

duced or transduced with LV.ADA2—were transplanted into immunodeficient NSGW41 mice. All animals remained healthy and steadily gained weight over the 20-week observation period, with no mortality or signs of toxicity, indicating that the treatment was well tolerated (Figure 4A).

At the endpoint, human hematopoietic engraftment—measured by the percentage of human CD45⁺ cells in the BM—was comparable among mice receiving LV.ADA2-transduced DADA2 cells, mock-transduced DADA2 cells, and mock-transduced HD controls (Figure 4B). VCN in the BM and spleen ranged between 3.62 ± 4.60 and 4.36 ± 6.26 , respectively (Figure 4C), and ADA2 protein expression was detected in human CD45⁺ BM cells from LV.ADA2 recipients (Figure 4D).

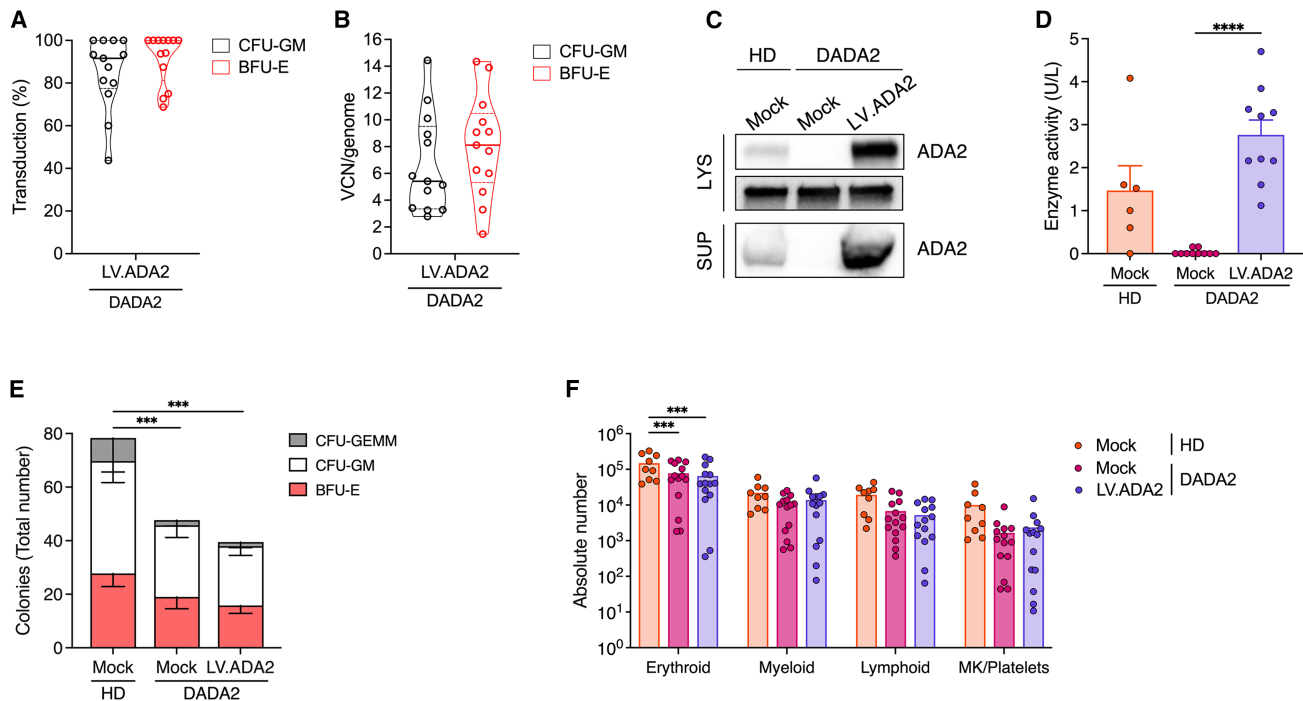


Figure 3. Lentiviral ADA2 transfer restores ADA2 expression and activity in DADA2 patient-derived CD34⁺ cells without impairing clonogenic or differentiation potential

(A) Transduction efficiency was assessed in BM-derived CD34⁺ cells from DADA2 patients following LV.ADA2 transduction at MOI 50, calculated as the percentage of vector-positive hematopoietic colonies (VCN \geq 0.5). (B) VCN per genome was measured in individual vector-positive erythroid (BFU-E) and myeloid (CFU-GM) colonies by droplet digital PCR. (C) Western blot analysis of ADA2 protein expression in cell lysates (Lys) and supernatants (Sup) from CD34⁺ patient-derived cells cultured *in vitro* for 14 days. Calnexin was used as a loading control. (D) ADA2 enzymatic activity measured in cell-free supernatants from HDs and patients cells cultured without vector (mock), and LV.ADA2-transduced patient cells. (E) Quantification of myeloid (CFU-GM), erythroid (BFU-E), and mixed-lineage (CFU-GEMM) colonies derived from mock- or LV.ADA2-transduced patient CD34⁺ cells, compared to mock-transduced HDs. (F) Absolute numbers of *in vitro*-differentiated erythroid, myeloid, lymphoid, and megakaryocyte/platelet cells obtained from 500 BM-derived CD34⁺ cells under mock (HD and DADA2) or LV.ADA2-transduced DADA2 CD34⁺ cells. Data are shown as mean \pm standard error of the mean. ***, $p < 0.001$. Lys, total cell protein extracts; Sup, cell supernatants.

The distribution of primitive HSCs and lineage-committed progenitors in mice receiving ADA2-corrected cells closely resembled that of HD controls (Figure 4E). While a modest, non-significant increase in PMN cell frequency was observed in mice receiving LV.ADA2 transduced patient cells compared to mice receiving mock transduced patient cells (Figure 4F), lymphoid differentiation remained unaffected (Figure 4G). Furthermore, hCD45⁺, mature myeloid and lymphoid populations—including monocytes, PMNs, B cells, T cells, and NK cells—were consistently detected in the peripheral blood of LV.ADA2-treated mice (Figures S5A and S5B), supporting preserved multilineage differentiation capacity.

Macroscopic examination of internal organs revealed no abnormalities. Histological examination of hematopoietic tissues (BM sternum and spleen), showed a similar degree of humanization, characterized by reconstitution of the splenic white pulp and BM with human immune cells across all experimental groups, with no evidence of inflammation, toxicity or proliferative lesions (Figure 4H).

Collectively, these findings demonstrate that LV.ADA2-mediated gene correction enables durable ADA2 expression and supports effective, multilineage hematopoietic reconstitution of DADA2 patient-derived HSPCs *in vivo*, with no detectable safety concerns.

Integration site profiling confirms genomic safety and polyclonal reconstitution of LV.ADA2-transduced patients' HSPCs

To comprehensively assess the clonal behavior and genomic safety of LV.ADA2-transduced cells, integration site (IS) profiles were analyzed across four experimental settings: (1) *in vitro*-expanded myeloid cells (Post-LC) obtained from mPB CD34⁺ cells from HDs transduced with LV.GFP or LV.ADA2; (2) total BM from NSGW41 mice transplanted with mPB-derived CD34⁺ cells from HD transduced with LV.GFP or LV.ADA2; (3) post-LC derived from transduced BM CD34⁺ cells of HDs and DADA2 patients; and (4) total BM from NSGW41 mice transplanted with LV.ADA2-transduced CD34⁺ cells from HDs or DADA2 patients.

In mPB-derived CD34⁺ cells from HDs, SLiM-PCR followed by high-throughput sequencing enabled the retrieval of hundreds to

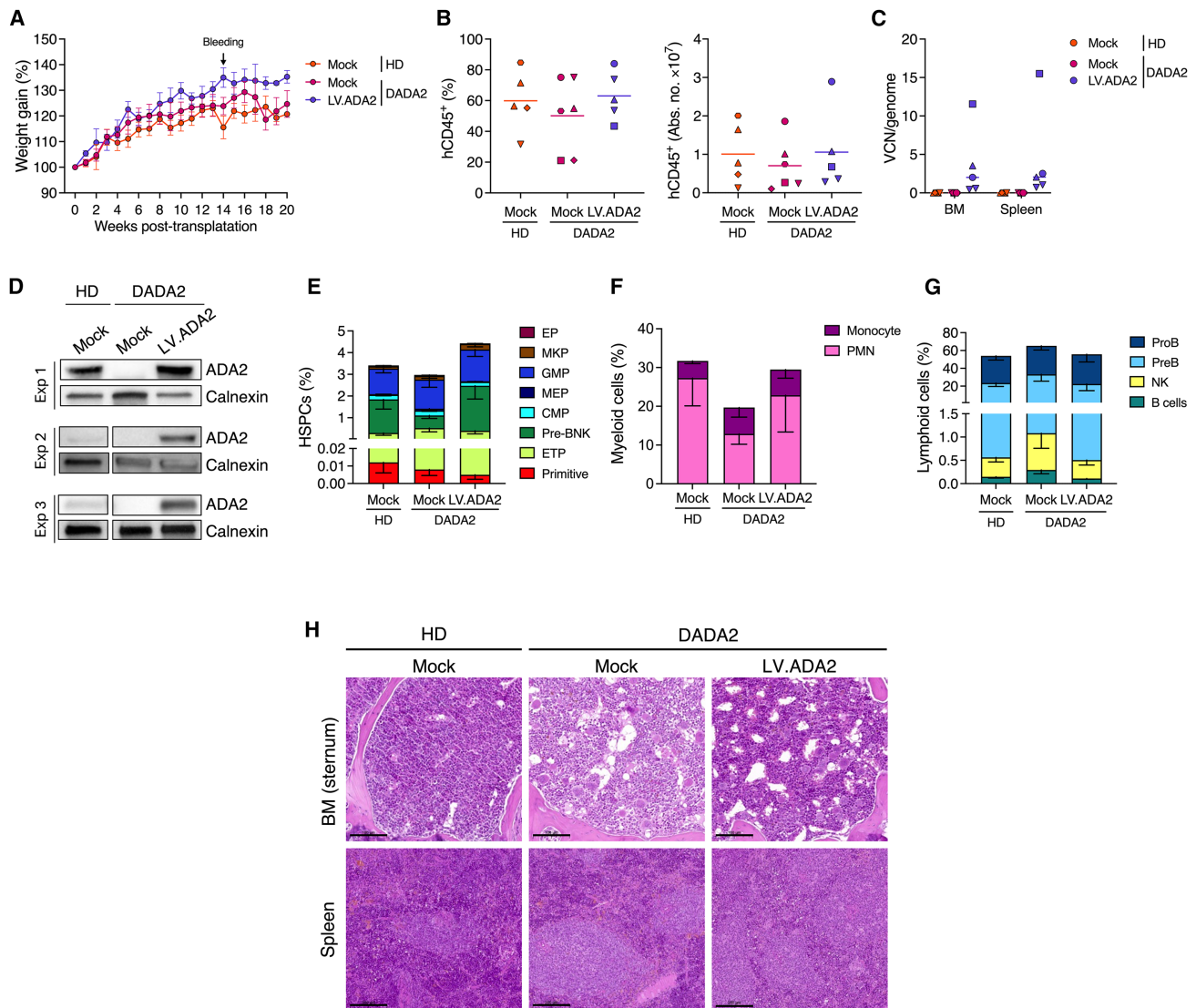


Figure 4. ADA2 gene correction supports long-term engraftment and multilineage differentiation of DADA2 patient-derived HSPCs in NSGW41 mice

(A) Time course analysis of body weight (% of initial weight) in NSGW41 mice transplanted with CD34⁺ cells from HDs and patients cultured without vector (mock), or LV.ADA2-transduced CD34⁺ cells from DADA2 patients. Mice were monitored up to 20 weeks post-transplant; the arrow indicates the peripheral blood sampling time point. (B) Human hematopoietic chimerism in the BM was assessed as both the percentage and absolute number of human CD45⁺ cells. (C) Average VCN per genome in total BM and spleen of mice receiving LV.ADA2-transduced CD34⁺ cells, measured 20 weeks post-transplant. (D) ADA2 protein expression in human CD45⁺ BM cells was evaluated by western blot in three independent experiments. (E–G) Frequencies of (E) HSPC subsets, (F) monocytes and polymorphonuclear (PMN) cells, and (G) lymphoid cells (B cells and NKT cells) in BM were quantified by multi-parametric flow cytometry across all groups. (H) Representative hematoxylin and eosin (H&E) staining of sternum BM and spleen sections from mice transplanted with HD mock, DADA2 mock, or LV.ADA2-transduced DADA2 CD34⁺ cells. Scale bars: 100 μ m in BM (sternum), 200 μ m in spleen. Data in B–G represent mean \pm standard error of the mean.

thousands ISs in both LV.GFP- and LV.ADA2-transduced samples in a dose-dependent manner (Table S1). As expected, the number of ISs retrieved from the BM of transplanted mice was lower than in the corresponding *in vitro* samples, although vector dose dependence was preserved. The number of ISs varied widely across HD and DADA2 donor samples, both *in vitro* (range: 158–7661) and *in vivo* (range: 15–1797), underscoring interindividual variability

in vector transduction efficiency and engraftment capacity in xenogeneic transplantation models (Table S2).

For safety purposes we evaluated the presence of common integration site (CIS) as possible readout of clonal selection for ISs targeting specific genes (Figures 5A and 5B). Moreover, analysis of clonal abundances *in vivo* showed that the vast majority of clones

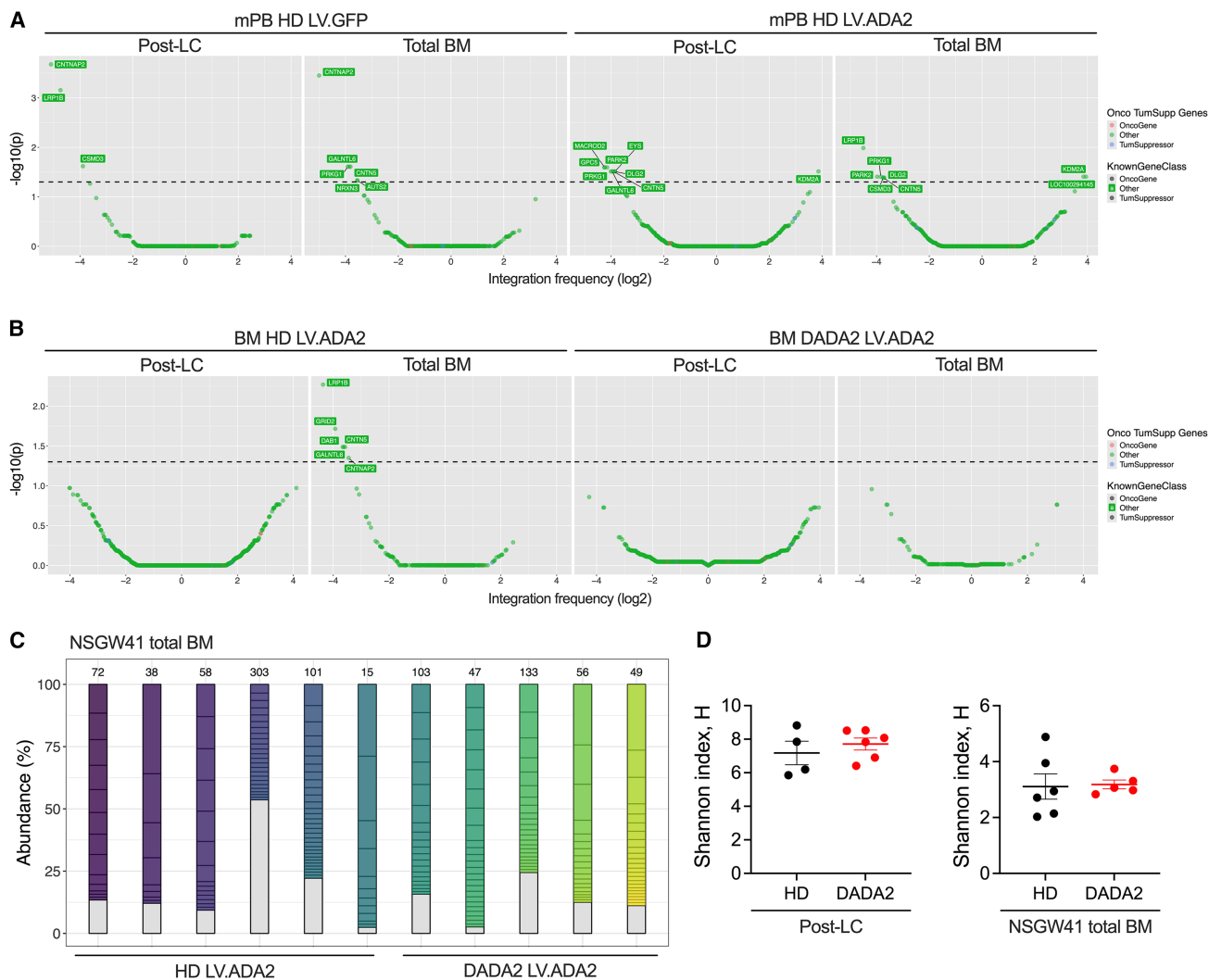


Figure 5. LV.ADA2 transduction supports polyclonal engraftment without evidence of clonal dominance

(A and B) Common integration site (CIS) analysis of integration site (IS) datasets from CD34⁺ cells transduced with either LV.GFP or LV.ADA2. CIS distributions are shown for (A) mPB-derived CD34⁺ cells from HDs and (B) *in vitro*-cultured CD34⁺-derived myeloid cells from HDs and DADA2 patients (Post-LC), as well as from total BM of NSGW41 mice transplanted with LV.ADA2-transduced CD34⁺ cells (Total BM). Each dot represents a gene; the x axis indicates the log₂-transformed integration frequency, and the y axis reports the significance of over-representation (Grubbs' test, $-\log_{10} p$ value). Genes classified as oncogenes are shown in red, tumor suppressors in blue, and all other genes in green, based on known gene annotations. (C) Stacked bar plots showing the relative abundance of individual ISs retrieved from total BM of NSGW41 mice transplanted with HD- or DADA2-derived CD34⁺ cells transduced with LV.ADA2. Each bar represents one recipient mouse. Colored segments correspond to individual clones contributing $\geq 1\%$ of the total IS pool. The number represent the total retrieved IS. (D) Shannon diversity index (H) quantifying clonal complexity *in vitro*-cultured CD34⁺ cells (post-LC) and total BM (*in vivo*), indicating consistently high diversity and absence of clonal skewing following LV.ADA2 transduction in patients' cells.

contributed at low frequency ($<1\%$), however, in some mice clones were well represented covering up to 30% of the entire IS repertoire (Figure 5C). These abundant ISs did not target proto-oncogenes or genes commonly linked to insertional mutagenesis, such as *LMO2*, *CCND2*, or *MECOM*, indicating a benign integration profile with no evidence of clonal selection.

Clonal diversity, measured by the Shannon diversity index, showed a high diversity in post-LC datasets (ranging from ~ 6

to ~ 9) while in mice it was reduced, ranging from 2 to 5, confirming the maintenance of polyclonality following long-term engraftment (Figure 5D).

Altogether, these findings from three independent experimental systems demonstrate that LV.ADA2 supports robust and polyclonal hematopoietic reconstitution without signs of clonal dominance or insertional risk, underscoring the favorable genomic safety profile of this therapeutic strategy.

DISCUSSION

This preclinical study demonstrates the biological efficacy and safety of a LV gene therapy approach for DADA2, a rare monogenic disorder caused by biallelic loss-of-function mutations in the *ADA2* gene. DADA2 is characterized by a broad and variable clinical spectrum, including systemic inflammation, vasculopathy, immunodeficiency, and progressive BMF.^{4,5} While anti-TNF therapy may offer partial control over inflammatory symptoms, it is ineffective for immunodeficiency and hematological manifestations.^{6,10} Allogeneic HSCT remains the only curative option for patients with hematologic involvement, but it carries substantial risks and is often limited by donor availability. Several reports have documented cases of post-transplant complications in DADA2 HSCT, including viral reactivations, graft-versus-host disease, autoimmune cytopenia, and declining chimerism.^{12–14} A recent systematic review indicated that 17 out of 25 DADA2 patients that underwent HSCT experienced post-transplant complications. Moreover, up to 20% of patients undergoing HSCT require a secondary transplant. These findings highlight the urgent need for alternative curative strategies, especially for patients without suitable donors or those at high risk of complications from intensive conditioning and post-transplant immunosuppression.

In this context, autologous gene therapy offers a compelling therapeutic alternative. By targeting patient-derived HSPCs, this strategy would avoid the risks of graft-versus-host disease and donor mismatch while potentially enabling durable correction of autoinflammation, immunodeficiency, and hematologic defects. In this study, we show that LV-mediated *ADA2* gene transfer into patient-derived HSPCs restores both protein expression and enzymatic activity while preserving clonogenic potential and multilineage differentiation *in vitro*.

Our work builds upon previous studies demonstrating that restoration of *ADA2* in mature macrophages results in correction of extracellular enzymatic activity and normalization of inflammatory profiles.^{3,18} However, those models did not address whether gene therapy at the HSPC level could enable durable hematopoiesis or long-term safety. Therefore, a key finding of this study is the capacity of gene-corrected patient HSPCs to retain robust, long-term multilineage hematopoietic reconstitution in immunodeficient mice, with engraftment levels and lineage output comparable to that of HD cells. Importantly, all key hematopoietic lineages, including B cells and neutrophils—lineages commonly affected in DADA2^{7,15,19–21}—were efficiently reconstituted *in vivo*. These results not only confirm preservation of stem cell multipotency but also demonstrate functional differentiation into clinically relevant effector populations. Importantly, *ADA2* protein was detected in human CD45⁺ cells isolated from the BM of transplanted mice at 20 weeks post-transplant, validating the *in vivo* stability of the transgene.

To evaluate these parameters, we employed the immunocompromised NSGW41 mouse strain, which lacks functional T, B, and

NK cells and carries the *Kit*^{W41} mutation that reduces endogenous hematopoiesis and supports sustained multilineage reconstitution without conditioning. Such immunocompromised models are widely used as a standard for assessing human HSPC function and, in this study, were applied to determine the efficacy and safety of *ADA2* gene correction rather than to reproduce DADA2 pathophysiology. Although we did not directly assess patients' phenotypes in humanized mice, but rather the capacity of patients' transduced CD34⁺ cells to engraft and differentiate, it is likely that this model is unsuitable to study DADA2 pathogenesis. Several factors may contribute to this limitation, including species-specific differences in *ADA2* biology and the absence of a direct rodent ortholog, as well as the profoundly immunodeficient background of NSGW41 mice, which restricts the establishment of a fully functional human immune system and prevents immune-endothelial interactions and inflammatory cues that drive vasculitis, cytopenias, and systemic inflammation in patients. Moreover, the murine BM niche and vascular microenvironment do not provide the conditions necessary to reveal hematopoietic and vascular abnormalities, and the relatively short time frame of xenotransplantation studies cannot capture the chronic and progressive course of DADA2 observed in humans.

A key highlight of our study is the demonstration that LV-*ADA2*-mediated correction enables restoration of both extracellular enzymatic activity and intracellular protein expression. Restoration of extracellular enzymatic activity is a key output given the correlation between disease severity and residual *ADA2* activity²² and the fact that HSCT is able to restore normal plasma *ADA2* activity, whilst correcting all disease manifestations.^{12,23} In addition, restoring intracellular protein expression might be relevant given the emerging evidence that intracellular *ADA2* might exert regulatory roles beyond its enzymatic activity.^{24,25} Together, these findings suggest that restoring *ADA2* expression in patients' CD34⁺ cells may be sufficient to support functional hematopoiesis both *in vitro* and *in vivo*, without compromising HSPC fitness. This work lays the foundation for a durable, autologous therapeutic strategy that could overcome the limitations of current treatments.

To evaluate safety and potential toxicity, we examined the effects of *ADA2* overexpression in HD-derived HSPCs, isolated from either mPB or BM.³ Transduced cells expanded normally, retained clonogenic capacity, and successfully engrafted in immunodeficient mice without evidence of toxicity, aberrant lineage output, or altered reconstitution of hematopoietic tissues. High levels of *ADA2* protein and enzymatic activity were maintained throughout the observation period, without affecting HSPC composition, myeloid output, or lymphoid development. These findings are particularly relevant to clinical translation, as they demonstrate that therapeutic *ADA2* expression in HSPCs does not compromise their fitness or induce hematopoietic skewing, thus supporting the safety of the LV-*ADA2* platform for autologous transplantation.

Our results also show that the current research-grade vector configuration drives normal to supranormal levels of ADA2 expression, with robust intracellular and extracellular protein expression. The expression was well tolerated in preclinical models and did not impair HSPC function or hematopoietic development. We further observed that the average LV.ADA2 VCN per genome was generally higher in patient-derived BM cells compared to HD-derived mPB cells. This difference might reflect a combination of biological and technical factors, including the different sources of CD34⁺ cells, the use of distinct vector production batches, and the intrinsic variability of primary HSPCs.

Achieving physiological expression may be sufficient for clinical efficacy, as disease correction has been observed in patients following successful HSCT^{13,23}. Increasing extracellular ADA2 enzymatic activity may offer an additional advantage over allogeneic HSCT. Our findings support the next phase of translational development, in which clinical-grade vector production and dosing studies will be essential to calibrate ADA2 expression, determine optimal therapeutic range, and align with the safety standards established in gene therapy trials for other monogenic disorders.¹⁷

The safety of LVs remains a critical consideration in the clinical development of gene therapies. To comprehensively evaluate the genomic safety and behavior of the LV.ADA2 construct, we performed high-resolution IS analysis across multiple experimental settings, recovering hundreds to thousands of unique ISs in all settings, with vector dose-dependent recovery observed in mPB-derived CD34⁺ cells from HDs. As expected, the number of ISs retrieved from *in vivo* samples was lower, reflecting the limited human cell output in xenogeneic recipients.²⁶ Nevertheless, clonal diversity remained high, and vector dose dependence was preserved. Across all conditions, integration events were widely distributed, without enrichment near proto-oncogenes, such as *LMO2*, *MECOM*, or *CCND2*, which have historically been associated with insertional oncogenesis in γ -retroviral vector trials.^{27–30}

Clonal diversity remained high with most individual clones contributing less than 1% to the total repertoire, and occasional high-abundance ISs (>30%) did not map to known oncogenic loci nor recur across recipients, indicating stochastic rather than selective clonal expansion. The Shannon diversity index confirmed preserved clonal heterogeneity *in vitro* and a moderate reduction *in vivo*—consistent with expected clonal contraction due to selective pressure in the xenogeneic niche, rather than vector-driven skewing. Notably, substantial inter-individual variability in IS numbers was observed, likely reflecting donor-specific differences in transduction efficiency and engraftment capacity, a factor to consider in clinical application. Overall, these findings support the genomic safety of the LV.ADA2 platform and are consistent with the well-characterized integration behavior of third-generation self-inactivating LVs currently used in clinical gene therapy trials for monogenic diseases, such as SCID, WAS, and MLD.^{31,32}

Taken together, our results establish a strong preclinical foundation for DADA2 gene therapy and align with the milestones that have enabled clinical translation of gene therapies for other inherited disorders. As with those studies, the transition from research-grade to GMP-grade manufacturing, determination of optimal vector dosing, and implementation of long-term follow-up studies will be essential next steps. Although *in vivo* efficacy could not be directly evaluated due to the lack of a murine ADA2 ortholog—and thus the absence of a relevant DADA2 disease model for gene therapy studies—our data provide compelling evidence of functional correction at the HSPC level based on *in vitro* and xenotransplantation studies. This represents a recognized challenge in the field of rare genetic diseases and underscores the value of integrating patient-derived cell models and humanized systems into the preclinical development pipeline.

In conclusion, our study provides compelling preclinical evidence that LV-mediated ADA2 gene correction is a viable, safe and effective strategy for restoring hematopoietic function in DADA2. By demonstrating robust engraftment, multilineage differentiation, and a favorable genomic safety profile, our findings support the continued clinical development of this approach. Future studies with clinical grade LV will be needed to establish the optimal level of ADA2 for phenotype correction and preclinical safety profile of HSPC in order progress to a clinical trial.

MATERIALS AND METHODS

Study approval and patient cohort

Patients were recruited from IRCCS San Raffaele Hospital (Milan, Italy) and IRCCS Ospedale Giannina Gaslini (Genoa, Italy). Diagnosis was based on pathologic or null ADA2 activity³³ and mutation analysis. Before sample collection, informed consent was obtained from patients or their parents. The study protocol RF-2019-12370600 entitled “Expanding the spectrum of adenosine deaminase 2 (ADA2) deficiency: toward a gene therapy approach” (Principal Investigator: M.G.) received approval from the ethics review boards of the participating institutes, ensuring compliance with the ethical principles outlined in the Declaration of Helsinki. Patients enrolled at the IRCCS San Raffaele Hospital also consented to the TIGET09 observational protocol for biological banking approved by the local ethical committee.

BM CD34⁺ cells were collected from patient 3 and patients 5–16, previously described in Bulté et al.⁷ The following patients were used for the humanized mouse experiments: patients 7, 9, 10, 12, 13, and 16. In addition, BM CD34⁺ cells from one previously undescribed patient were included. This patient is a female carrying compound heterozygous ADA2 variants (p.Ala45Thr/p.Tyr453Cys) and presenting with cutaneous vasculitis manifestations, including livedo reticularis, consistent with an inflammatory phenotype. At the time of BM aspirate, the patient was under treatment with the TNF inhibitor etanercept.

Isolation of CD34⁺ cells

Granulocyte colony-stimulating factor (G-CSF) and plerixafor-mobilized peripheral blood (mPB) CD34⁺ HSPCs from HDs were

purified in-house from Mobilized Leukopaks (AllCells) using the CliniMACS CD34 reagent system (Miltenyi Biotec), according to the TIGET-HPCT protocol approved by OSR Ethical Committee and following the manufacturer's instructions. For DADA2 patients, CD34⁺ HSPCs were isolated from BM aspirates. BM was diluted 1:1 with sterile PBS and carefully layered over Lymphoprep density gradient medium. Following centrifugation at 1,800 rpm for 20 min (brake off), BM mononuclear cells were collected, washed with PBS, and subjected to red blood cell lysis using ammonium-chloride-potassium buffer. After an additional wash, cells were re-suspended in MACS buffer (Miltenyi Biotec), and CD34⁺ cells were isolated using the CD34 MicroBead Kit UltraPure (Miltenyi Biotec, Cat. 130046702). BM-derived CD34⁺ cells from HDs were obtained from Lonza.

Lentiviral transduction of CD34⁺ cells

CD34⁺ cells were plated at a density of 10⁶ cells/mL in wells pre-coated with RetroNectin (2 µg/cm²; Takara Bio) in serum-free CellGro medium (CellGenix) supplemented with 1% l-glutamine, 1% penicillin/streptomycin, human stem cell factor (hSCF; 300 ng/mL), human thrombopoietin (hTPO; 100 ng/mL), human Fms-like tyrosine kinase 3 ligand (hFLT3L; 300 ng/mL), and human interleukin-3 (hIL-3; 60 ng/mL; all from PeproTech). After 22 h of prestimulation, cells were incubated with 16,16-dimethyl prostaglandin E2 (PGE₂; 10 µM; Cayman Chemical) for 2 h, followed by overnight transduction with either Mock (cells cultured without vector), LV.ADA2 or LV.GFP³ at a multiplicity of infection of 25 or 50. CD34⁺ cells from DADA2 patients were transduced with LV.ADA2 at MOI 50. Following a 14-h transduction, cells were collected, washed, and cultured in IMDM supplemented with fetal bovine serum (FBS), 1% L-glutamine, 1% penicillin/streptomycin, hSCF (100 ng/mL), hTPO (100 ng/mL), hFLT3L (100 ng/mL), and hIL-3 (20 ng/mL) for up to 14 days.

Xenotransplantation assay

To study *in vivo* engraftment and long-term repopulating potential of transduced cells, we used the NOD.Cg-Kit^{W-41}Prkdc^{scid}Il2rg^{tm1Wjl}/WaskJ mice (NSGW41)³⁴ mouse strain. Mice were maintained under specific pathogen-free conditions at the IRCCS San Raffaele Scientific Institute Animal Facility. All animal procedures were approved by the Institutional Animal Care and Use Committee (IACUC no. 1186) and conducted in accordance with Italian Ministry of Health guidelines for the care and use of experimental animals. All efforts were made to minimize the number of animals used and to reduce pain or distress during and after the procedures.

For transplantation, 200,000 CD34⁺ cells isolated from HD mobilized peripheral blood (mPB), either mock-transduced or transduced with LV.ADA2 or LV.GFP at a multiplicity of infection of 25 or 50, were injected intravenously into 8-week-old female NSGW41 mice. In experiments using patient-derived HSPCs, 100,000–250,000 BM CD34⁺ cells (HD mock, DADA2 mock, or DADA2 LV.ADA2-transduced at MOI 50) were adoptively transferred into 7–8-week-old female mice. Human cell engraftment in peripheral blood (PB) was

monitored periodically by tail vein blood sampling. Mice were euthanized 18 or 20 weeks post-transplantation. At the time of sacrifice, BM cells were harvested by flushing femurs and tibiae.

Human hematopoietic chimerism in BM and PB was evaluated using a whole-blood dissection cytometry assay previously described.^{7,35} Propidium iodide (BioLegend) was used to assess cell viability, and FlowCount beads (BD Biosciences) were added to perform absolute cell quantification. All samples were acquired using BD FACSymphony A5 (BD Biosciences), calibrated with Rainbow beads (Sperotech, Lake Forest, Ill). Raw data were collected using DIVA software and subsequently analyzed with FlowJo software.

To evaluate the long-term clonogenic potential of engrafted human HSPCs, we isolated the human CD45⁺ fraction from total murine BM and plated 100,000 cells per dish. After 14 days of incubation, colonies were scored by light microscopy. The following colony types were identified and quantified: erythroid burst-forming units (BFU-E) and granulocyte-macrophage colony-forming units (CFU-GM).

Colony forming unit assay

Following the 14-h transduction, CD34⁺ cells were resuspended in complete MethoCult H4434 medium (Stemcell Technologies) and plated in triplicate in 35-mm culture dishes at a density of 500 cells per dish. After 14 days of incubation, colonies were scored by light microscopy. The following colony types were identified and quantified: erythroid burst-forming units (BFU-E), granulocyte-macrophage colony-forming units (CFU-GM), and multilineage colonies containing granulocytes, erythrocytes, monocytes/macrophages, and megakaryocytes (CFU-GEMM).

Measurement of vector copy number and transduction efficiency

Genomic DNA was extracted from cells 14 days post-transduction using the QIAamp DNA Mini Kit (Qiagen), according to the manufacturer's instructions. For single-colony analysis, individual CFUs were manually picked and lysed using QuickExtract DNA Extraction Solution (Lucigen Corporation). Vector copy number (VCN) per diploid genome was quantified by droplet digital PCR on a QX200 Droplet Digital PCR System (Bio-Rad). The following primers and probe were used to detect integrated LVs: HIV probe, 5'-FAM-ATCTCTCTCCTTCTAGCCTC-MGBNFQ-3'; HIV forward primer, 5'-TACTGACGCTCTCGCACC-3'; HIV reverse primer, 5'-TCTCGACGCAGACTCG-3'. GAPDH was used as a reference for the diploid genome using a 20× primer/probe mix (Bio-Rad, Cat. #10031244, Assay ID: dHsaCP2506596). Colonies were classified as vector-positive if the VCN was ≥0.5 copies per genome. Transduction efficiency was calculated as the percentage of vector-positive colonies relative to the total number of analyzed colonies.

In vitro differentiation assay

In vitro differentiation was performed as previously described.³⁶ Briefly, non-tissue culture-treated 96-well flat-bottom plates were coated with StemSpan Differentiation Coating Material (Stemcell

Technologies) for 2 h prior to cell seeding, BM-derived CD34⁺ cells from HDs or DADA2 patients, either mock-or LV.ADA2-transduced, were seeded in SFEM II medium (Stemcell Technologies) supplemented with the following cytokines and growth factors: hSCF (100 ng/mL), hFLT3 (10 ng/mL), hIL-7 (100 ng/mL), hIL-2 (10 ng/mL; Novartis, Basel, Switzerland), hTPO (75 ng/mL), hIL-6 (40 ng/mL), hIL-3 (10 ng/mL), hIL-11 (50 ng/mL), hEPO (0.1 U/mL; PeproTech, Cranbury, NJ), hIL-4 (10 ng/mL; Miltenyi Biotec), and hLDL (4 mg/mL; Stemcell Technologies). Culture medium was refreshed every 3–4 days. After 3 weeks, cells were harvested and stained with fluorescently labeled antibodies as described by Bulté and colleagues.⁷ All antibodies were purchased from BioLegend or BD Biosciences. FlowCount beads (BD Biosciences) were added to enable absolute cell quantification. Samples were acquired on a BD FACSymphony A5 flow cytometer (BD Biosciences), calibrated with Rainbow Calibration Particles (Spherotech). Raw data were collected using BD FACSDiva software and analyzed with FlowJo software.

Western blot analysis

Proteins were extracted using ice-cold RIPA buffer containing 150 mM NaCl, 20 mM Tris-HCl (pH 7.4), 1 mM EDTA, 1 mM sodium orthovanadate, 1 mM PMSF, and protease inhibitors (10 µg/mL aprotinin and 10 µg/mL leupeptin). Protein concentrations were determined using the Bio-Rad Protein Assay Dye Reagent Concentrate (Bio-Rad, Cat. #5000006). Equal amounts of total protein (30–45 µg) were resolved on 10%–12% SDS-PAGE gels (Bio-Rad).

For analysis of secreted proteins, cell-free supernatants were precipitated by mixing with cold acetone at a 1:4 ratio and incubating at –20°C for at least 1 h. Samples were centrifuged at 15,000 rpm for 15 min at 4°C. The resulting pellets were resuspended in Laemmli buffer.

Proteins were transferred to Trans-Blot Turbo PVDF membranes (0.2 µm; Bio-Rad, Cat. #1704156) using the Trans-Blot Turbo Transfer System (Bio-Rad). Membranes were blocked for one hour in TBS containing 5% skimmed milk and 0.05% Tween 20, followed by overnight incubation at 4°C with primary antibodies: anti-ADA2 (1:500; Cat. HPA007888 Sigma-Aldrich), anti-calnexin (1:1500; Cat. #C4731 Sigma-Aldrich). After washing, membranes were incubated with HRP-conjugated secondary antibodies. Signal detection was performed using the Immobilon Western Chemiluminescent HRP Substrate (WBKLS, Millipore), and blot images were acquired using the iBright FL1500 Imaging System (Thermo Fisher Scientific).

ADA2 activity measurement

ADA2 enzymatic activity in plasma and cell culture supernatants was measured using a previously described automated spectrophotometric assay that quantifies the adenosine-dependent generation of ammonia in the presence of a selective ADA1 inhibitor, EHNA (erythro-9-Amino-β-hexyl-α-methyl-9H-purine-9-ethanol hydrochloride; Cayman Chemical).³⁷ Reactions were carried out in

96-well plates, and absorbance was measured using a FLUOstar Omega Microplate Reader (BMG Labtech).

Histopathological analysis

Spleen and sternal BM samples were fixed in 10% neutral buffered formalin, trimmed, embedded in paraffin wax, and sectioned at 3 µm thickness. Sections were stained with Hematoxylin and Eosin (H&E) for histopathological examination. Lesions were graded on a semi-quantitative scale from 1 to 5, defined as follows: minimal (1), mild (2), moderate (3), marked (4), and severe (5), with “minimal” indicating the lowest discernible degree and “severe” indicating the highest. Histopathological examination was performed by a board-certified veterinary pathologist.

Statistical methods

Differences among three or more independent groups were assessed using the nonparametric Kruskal-Wallis test. Paired group comparisons were analyzed with the Wilcoxon signed-rank test. For experiments involving two independent variables, a two-way ANOVA was used to evaluate main effects and interactions. Data normality was assessed using the Shapiro-Wilk test prior to ANOVA. When appropriate, post hoc comparisons were conducted using Tukey’s multiple comparison test. *p* values ≤0.05 were considered statistically significant. All statistical analyses and data visualizations were performed using GraphPad Prism version 10 (GraphPad Software).

DATA AND CODE AVAILABILITY

All data generated in this study are openly available in the Zenodo repository at <https://doi.org/10.5281/zenodo.17130716>.

ACKNOWLEDGMENTS

We thank Claudia Sartirana and Alessandro Romano for technical assistance, Rossana Norata and Martina Rocchi for tissue specimen processing, Patrizia Cristofori for critical review of pathology data, SR-Tiget Processing Developmental Lab for LV preparations.

We thank Claudia Waskow for her advice in handling NSGW41 mice.

IRCCS San Raffaele Scientific Institute, IRCCS Istituto Giannina Gaslini, and IRCCS Bambino Gesù Children’s Hospital are part of the European Reference Network for Rare Immunodeficiency, Autoinflammatory and Autoimmune Diseases, ERN-RITA (Project ID 739543). IRCCS San Raffaele Scientific Institute is part of the Inborn Error Working Party of The European Society for Blood and Marrow Transplantation (EBMT). The centers involved are part of the Italian Pediatric Onco-Hematology Association (AIEOP), and clinicians are members of the Associazione Italiana Immunodeficienze (ImmunITA). A.A. is the recipient of Else Kröner-Fresenius-Stiftung (EKFS) prize.

This work supported by Fondazione Telethon ETS (SR-Tiget Core grant, Tele21-A5) to AM, the Italian Ministry of Health (Progetto Ricerca Finalizzata 2019, RF-2019-12370600) to M.G., C.D., A.M., and A.A., PNRR 2022 (PNRR-MR1-2022-12376594) to F.B. and A.A., and the Else Kröner-Fresenius-Stiftung (EKFS) prize for Medical Research 2020 to A.A. Fondazione Telethon ETS has obtained Orphan Drug Designation (EU/3/21/2496) for the medicinal product “Autologous CD34⁺ cell enriched population containing hematopoietic stem and progenitor cells transduced *ex vivo* with a lentiviral vector encoding the human ADA2 gene.”

C.R. conducted this study as partial fulfillment of her Ph.D in Molecular Medicine, Gene and Cell Therapy program at Vita-Salute San Raffaele University, Milan, Italy.

AUTHOR CONTRIBUTIONS

Study design: C.R., D.B., and A.M.; perform experiments: C.R., D.B., C.M.-N., E.P., and P.Q.; data interpretation: C.R., D.B., C.M.-N., and A.M.; flow cytometry sample acquisition and analysis: C.R., D.B., and L.B.-R.; patients' recruitment, management, and performed procedures: F. Barzaghi, C.V., R.C., F.S., M.L., S.F., A.I., F.D.B., M.M., F.C., M.P.C., M.G.M., C.D., and A.A.; pathological assessment: S.D.I. and F.S.; integration site analysis: F.G., F. Benedicenti, S.A., and E.M.; manuscript writing: C.R. and A.M.; critical review of the manuscript: D.B., S.S., and A.A.; funding acquisition: M.G., C.D., A.A., and A.M.; work coordination: A.M. All authors have read the manuscript and agree to all its contents.

DECLARATION OF INTERESTS

Authors declare no conflicts of interest.

SUPPLEMENTAL INFORMATION

Supplemental information can be found online at <https://doi.org/10.1016/j.omtm.2025.101624>.

REFERENCES

- Zhou, Q., Yang, D., Ombrello, A.K., Zavialov, A.V., Toro, C., Zavialov, A.V., Stone, D.L., Chae, J.J., Rosenzweig, S.D., Bishop, K., et al. (2014). Early-onset stroke and vasculopathy associated with mutations in ADA2. *N. Engl. J. Med.* 370, 911–920. <https://doi.org/10.1056/NEJMoa1307361>.
- Navon Elkan, P., Pierce, S.B., Segel, R., Walsh, T., Barash, J., Padeh, S., Zlotogorski, A., Berkun, Y., Press, J.J., Mukamel, M., et al. (2014). Mutant adenosine deaminase 2 in a polyarteritis nodosa vasculopathy. *N. Engl. J. Med.* 370, 921–931. <https://doi.org/10.1056/NEJMoa1307362>.
- Zoccolillo, M., Brigida, I., Barzaghi, F., Scala, S., Hernández, R.J., Basso-Ricci, L., Colantuoni, M., Pettinato, E., Sergi, L.S., Milardi, G., et al. (2021). Lentiviral correction of enzymatic activity restrains macrophage inflammation in adenosine deaminase 2 deficiency. *Blood Adv.* 5, 3174–3187. <https://doi.org/10.1182/bloodadvances.2020003811>.
- Barron, K.S., Aksentijevich, I., Deutch, N.T., Stone, D.L., Hoffmann, P., Videgar-Laird, R., Soldatos, A., Bergerson, J., Toro, C., Cudrici, C., et al. (2021). The Spectrum of the Deficiency of Adenosine Deaminase 2: An Observational Analysis of a 60 Patient Cohort. *Front. Immunol.* 12, 811473. <https://doi.org/10.3389/fimmu.2021.811473>.
- Maccora, I., Maniscalco, V., Campani, S., Carrera, S., Abbati, G., Marrani, E., Mastrolia, M.V., and Simonini, G. (2023). A wide spectrum of phenotype of deficiency of deaminase 2 (DADA2): a systematic literature review. *Orphanet J. Rare Dis.* 18, 117. <https://doi.org/10.1186/s13023-023-02721-6>.
- Michniacki, T.F., Hannibal, M., Ross, C.W., Frame, D.G., DuVall, A.S., Khoriaty, R., Vander Lugt, M.T., and Walkovich, K.J. (2018). Hematologic Manifestations of Deficiency of Adenosine Deaminase 2 (DADA2) and Response to Tumor Necrosis Factor Inhibition in DADA2-Associated Bone Marrow Failure. *J. Clin. Immunol.* 38, 166–173. <https://doi.org/10.1007/s10875-018-0480-4>.
- Bulte, D., Barzaghi, F., Mesa-Nunez, C., Rigamonti, C., Basso-Ricci, L., Viscconti, C., Crippa, S., Pettinato, E., Gilioli, D., Milani, R., et al. (2025). Early bone marrow alterations in patients with adenosine deaminase 2 deficiency across disease phenotypes and severities. *J. Allergy Clin. Immunol.* 155, 616–627.e618. <https://doi.org/10.1016/j.jaci.2024.09.007>.
- Lee, P.Y., Davidson, B.A., Abraham, R.S., Alter, B., Arostegui, J.I., Bell, K., Belot, A., Bergerson, J.R.E., Bernard, T.J., Brogan, P.A., et al. (2023). Evaluation and Management of Deficiency of Adenosine Deaminase 2: An International Consensus Statement. *JAMA Netw. Open* 6, e2315894. <https://doi.org/10.1001/jamanetworkopen.2023.15894>.
- Meyts, I., and Aksentijevich, I. (2018). Deficiency of Adenosine Deaminase 2 (DADA2): Updates on the Phenotype, Genetics, Pathogenesis, and Treatment. *J. Clin. Immunol.* 38, 569–578. <https://doi.org/10.1007/s10875-018-0525-8>.
- Deutch, N.T., Yang, D., Lee, P.Y., Yu, X., Moura, N.S., Schnappauf, O., Ombrello, A.K., Stone, D., Kuehn, H.S., Rosenzweig, S.D., et al. (2022). TNF inhibition in vasculitis management in adenosine deaminase 2 deficiency (DADA2). *J. Allergy Clin. Immunol.* 149, 1812–1816.e6. <https://doi.org/10.1016/j.jaci.2021.10.030>.
- Van Eyck, L., Jr., Hershfield, M.S., Pombal, D., Kelly, S.J., Ganson, N.J., Moens, L., Frans, G., Schaballie, H., De Hertogh, G., Dooley, J., et al. (2015). Hematopoietic stem cell transplantation rescues the immunologic phenotype and prevents vasculopathy in patients with adenosine deaminase 2 deficiency. *J. Allergy Clin. Immunol.* 135, 283–297.e5. <https://doi.org/10.1016/j.jaci.2014.10.010>.
- Hashem, H., Kumar, A.R., Müller, I., Babor, F., Bredius, R., Dalal, J., Hsu, A.P., Holland, S.M., Hickstein, D.D., Jolles, S., et al. (2017). Hematopoietic stem cell transplantation rescues the hematological, immunological, and vascular phenotype in DADA2. *Blood* 130, 2682–2688. <https://doi.org/10.1182/blood-2017-07-798660>.
- Hashem, H., Buccioli, G., Ozen, S., Unal, S., Bozkaya, I.O., Akarsu, N., Taskinen, M., Koskenvuo, M., Saarela, J., Dimitrova, D., et al. (2021). Hematopoietic Cell Transplantation Cures Adenosine Deaminase 2 Deficiency: Report on 30 Patients. *J. Clin. Immunol.* 41, 1633–1647. <https://doi.org/10.1007/s10875-021-01098-0>.
- Hashem, H., Dimitrova, D., and Meyts, I. (2022). Allogeneic Hematopoietic Cell Transplantation for Patients With Deficiency of Adenosine Deaminase 2 (DADA2): Approaches, Obstacles and Special Considerations. *Front. Immunol.* 13, 932385. <https://doi.org/10.3389/fimmu.2022.932385>.
- Barzaghi, F., Cicalese, M.P., Zoccolillo, M., Brigida, I., Barcella, M., Merelli, I., Sartirana, C., Zanussi, M., Calbi, V., Bernardo, M.E., et al. (2022). Case Report: Consistent disease manifestations with a staggered time course in two identical twins affected by adenosine deaminase 2 deficiency. *Front. Immunol.* 13, 910021. <https://doi.org/10.3389/fimmu.2022.910021>.
- Barzaghi, F., Minniti, F., Mauro, M., Bortoli, M.D., Balter, R., Bonetti, E., Zaccaron, A., Vitale, V., Omrani, M., Zoccolillo, M., et al. (2018). ALPS-Like Phenotype Caused by ADA2 Deficiency Rescued by Allogeneic Hematopoietic Stem Cell Transplantation. *Front. Immunol.* 9, 2767. <https://doi.org/10.3389/fimmu.2018.02767>.
- Tucci, F., Scaramuzza, S., Aiuti, A., and Mortellaro, A. (2021). Update on Clinical Ex Vivo Hematopoietic Stem Cell Gene Therapy for Inherited Monogenic Diseases. *Mol. Ther.* 29, 489–504. <https://doi.org/10.1016/j.ymthe.2020.11.020>.
- Hong, Y., Casimir, M., Houghton, B.C., Zhang, F., Jensen, B., Omoyinmi, E., Torrance, R., Papadopoulou, C., Cummins, M., Roderick, M., et al. (2022). Lentiviral Mediated ADA2 Gene Transfer Corrects the Defects Associated With Deficiency of Adenosine Deaminase Type 2. *Front. Immunol.* 13, 852830. <https://doi.org/10.3389/fimmu.2022.852830>.
- Suleyman, M., Tan, C., Uner, A., Inkaya, C., Aytac, S., Buyukasik, Y., Boztug, K., Tezcan, I., and Cagdas, D. (2022). Adenosine Deaminase Type II Deficiency: Severe Chronic Neutropenia, Lymphoid Infiltration in Bone Marrow, and Inflammatory Features. *Immunol. Investig.* 51, 558–566. <https://doi.org/10.1080/08820139.2020.1853153>.
- Yap, J.Y., Moens, L., Lin, M.W., Kane, A., Kelleher, A., Toong, C., Wu, K.H.C., Sewell, W.A., Phan, T.G., Hollway, G.E., et al. (2021). Intrinsic Defects in B Cell Development and Differentiation, T Cell Exhaustion and Altered Unconventional T Cell Generation Characterize Human Adenosine Deaminase Type 2 Deficiency. *J. Clin. Immunol.* 41, 1915–1935. <https://doi.org/10.1007/s10875-021-01141-0>.
- Schena, F., Penco, F., Volpi, S., Pastorino, C., Caorsi, R., Kalli, F., Fenoglio, D., Salis, A., Bertoni, A., Prigione, I., et al. (2021). Dysregulation in B-cell responses and T follicular helper cell function in ADA2 deficiency patients. *Eur. J. Immunol.* 51, 206–219. <https://doi.org/10.1002/eji.202048549>.
- Lee, P.Y., Kellner, E.S., Huang, Y., Furutani, E., Huang, Z., Bainter, W., Alosaimi, M.F., Stafstrom, K., Platt, C.D., Stauber, T., et al. (2020). Genotype and functional correlates of disease phenotype in deficiency of adenosine deaminase 2 (DADA2). *J. Allergy Clin. Immunol.* 145, 1664–1672.e10. <https://doi.org/10.1016/j.jaci.2019.12.908>.
- Buccioli, G., Delafontaine, S., Segers, H., Bossuyt, X., Hershfield, M.S., Moens, L., and Meyts, I. (2017). Hematopoietic Stem Cell Transplantation in ADA2 Deficiency: Early Restoration of ADA2 Enzyme Activity and Disease Relapse upon Drop of Donor Chimerism. *J. Clin. Immunol.* 37, 746–750. <https://doi.org/10.1007/s10875-017-0449-8>.
- Greiner-Tollersrud, O.K., Krausz, M., Boehler, V., Polyzou, A., Seidl, M., Spahiu, A., Abdullah, Z., Andryka-Cegielski, K., Dominick, F.I., Huebscher, K., et al. (2024). ADA2 is a lysosomal deoxyadenosine deaminase acting on DNA involved in regulating TLR9-mediated immune sensing of DNA. *Cell Rep.* 43, 114899. <https://doi.org/10.1016/j.celrep.2024.114899>.

25. Dong, L., Luo, W., Maksym, S., Robson, S.C., and Zavialov, A.V. (2024). Adenosine deaminase 2 regulates the activation of the toll-like receptor 9 in response to nucleic acids. *Front. Med.* 18, 814–830. <https://doi.org/10.1007/s11684-024-1067-5>.
26. Biffi, A., Montini, E., Lorioli, L., Cesani, M., Fumagalli, F., Plati, T., Baldoli, C., Martino, S., Calabria, A., Canale, S., et al. (2013). Lentiviral hematopoietic stem cell gene therapy benefits metachromatic leukodystrophy. *Science* 341, 1233–1238. <https://doi.org/10.1126/science.1233158>.
27. Howe, S.J., Mansour, M.R., Schwarzwald, K., Bartholomae, C., Hubank, M., Kempinski, H., Brugman, M.H., Pike-Overzet, K., Chatters, S.J., de Ridder, D., et al. (2008). Insertional mutagenesis combined with acquired somatic mutations causes leukemogenesis following gene therapy of SCID-X1 patients. *J. Clin. Investig.* 118, 3143–3150. <https://doi.org/10.1172/JCI35798>.
28. Hacein-Bey-Abina, S., Von Kalle, C., Schmidt, M., McCormack, M.P., Wulffraat, N., Leboulch, P., Lim, A., Osborne, C.S., Pawliuk, R., Morillon, E., et al. (2003). LMO2-associated clonal T cell proliferation in two patients after gene therapy for SCID-X1. *Science* 302, 415–419. <https://doi.org/10.1126/science.1088547>.
29. Montini, E., Cesana, D., Schmidt, M., Sanvito, F., Bartholomae, C.C., Ranzani, M., Benedicenti, F., Sergi, L.S., Ambrosi, A., Ponzoni, M., et al. (2009). The genotoxic potential of retroviral vectors is strongly modulated by vector design and integration site selection in a mouse model of HSC gene therapy. *J. Clin. Investig.* 119, 964–975. <https://doi.org/10.1172/JCI37630>.
30. Deichmann, A., Hacein-Bey-Abina, S., Schmidt, M., Garrigue, A., Brugman, M.H., Hu, J., Glimm, H., Gyapay, G., Prum, B., Fraser, C.C., et al. (2007). Vector integration is nonrandom and clustered and influences the fate of lymphopoiesis in SCID-X1 gene therapy. *J. Clin. Investig.* 117, 2225–2232. <https://doi.org/10.1172/JCI31659>.
31. Calabria, A., Spinozzi, G., Cesana, D., Buscaroli, E., Benedicenti, F., Pais, G., Gazzo, F., Scala, S., Lidonnici, M.R., Scaramuzza, S., et al. (2024). Long-term lineage commitment in haematopoietic stem cell gene therapy. *Nature* 636, 162–171. <https://doi.org/10.1038/s41586-024-08250-x>.
32. Montini, E., Naldini, L., Booth, C., Kohn, D.B., and Aiuti, A. (2025). Balancing efficacy and safety in lentiviral vector-mediated hematopoietic stem cell gene therapy. *Mol. Ther.* 33, 6–8. <https://doi.org/10.1016/j.ymthe.2024.12.028>.
33. Cafaro, A., Pigliasco, F., Barco, S., Penco, F., Schena, F., Caorsi, R., Volpi, S., Tripodi, G., Gattorno, M., and Cangemi, G. (2021). A Novel LC-MS/MS-Based Method for the Diagnosis of ADA2 Deficiency from Dried Plasma Spot. *Molecules* 26, 5707. <https://doi.org/10.3390/molecules26185707>.
34. Rahmig, S., Kronstein-Wiedemann, R., Fohgrub, J., Kronstein, N., Nevmerzhitskaya, A., Bornhäuser, M., Gassmann, M., Platz, A., Ordemann, R., Tonn, T., and Waskow, C. (2016). Improved Human Erythropoiesis and Platelet Formation in Humanized NSGW41 Mice. *Stem Cell Rep.* 7, 591–601. <https://doi.org/10.1016/j.stemcr.2016.08.005>.
35. Basso-Ricci, L., Scala, S., Milani, R., Migliavacca, M., Rovelli, A., Bernardo, M.E., Ciceri, F., Aiuti, A., and Biasco, L. (2017). Multiparametric Whole Blood Dissection: A one-shot comprehensive picture of the human hematopoietic system. *Cytometry. A* 91, 952–965. <https://doi.org/10.1002/cyto.a.23148>.
36. Scala, S., Ferrua, F., Basso-Ricci, L., Dionisio, F., Omrani, M., Quaranta, P., Jofra Hernandez, R., Del Core, L., Benedicenti, F., Monti, I., et al. (2023). Hematopoietic reconstitution dynamics of mobilized- and bone marrow-derived human hematopoietic stem cells after gene therapy. *Nat. Commun.* 14, 3068. <https://doi.org/10.1038/s41467-023-38448-y>.
37. Lee, P.Y., Schulert, G.S., Canna, S.W., Huang, Y., Sundel, J., Li, Y., Hoyt, K.J., Blaustein, R.B., Wactor, A., Do, T., et al. (2020). Adenosine deaminase 2 as a biomarker of macrophage activation syndrome in systemic juvenile idiopathic arthritis. *Ann. Rheum. Dis.* 79, 225–231. <https://doi.org/10.1136/annrheumdis-2019-216030>.

Supplemental information

Gene therapy supports long-term reconstitution of patient hematopoietic stem cells in deficiency of adenosine deaminase 2

Chiara Rigamonti, Dimitri Bulté, Federica Barzaghi, Cristina Mesa-Nuñez, Luca Basso-Ricci, Emanuela Pettinato, Camilla Visconti, Sara Degl'Innocenti, Francesco Gazzo, Fabrizio Benedicenti, Sergio Arévalo, Pamela Quaranta, Francesca Sanvito, Roberta Caorsi, Francesca Schena, Michela Lupia, Silvia Federici, Antonella Insalaco, Fabrizio De Benedetti, Serena Scala, Maurizio Miano, Francesca Conti, Maria Pia Cicalese, Eugenio Montini, Marco Gattorno, Carlo Dufour, Alessandro Aiuti, and Alessandra Mortellaro

SUPPLEMENTAL MATERIALS

SUPPLEMENTAL METHODS

Vector integration site retrieval and sequencing

Genomic DNA was extracted from human BM and mPB CD34+ cells, and from BM samples harvested from NSGW41 mice. Integration site (IS) retrieval was performed using Sonication Linker-mediated PCR (SLiM-PCR), as previously described^{1,2}. Briefly, ~30 ng of genomic DNA per sample was sonicated and split into three technical replicates. Fragmented DNA was then end-repaired, adenylated, and ligated to a linker cassette using the NEBNext® Ultra™ II DNA Library Prep Kit (New England Biolabs, Cat. n° E7645), following the manufacturer's instruction. Two consecutive PCR amplifications (25 and 10 cycles, respectively) were performed using primers targeting the vector Long Terminal Repeats (LTR) and the linker cassette to selectively amplify vector–genome junctions. Clean-up and concentration steps were included between the two PCR rounds to optimize second amplification.

Primers used in this protocol included sample-specific barcodes and sequencing adapters for multiplexed paired-end sequencing on the MGI platforms. Detailed primer sequences and barcoding information have been previously published¹. A single sequencing library comprising 145 samples was generated and sequenced using the MGI G400 platform, yielding $>1.96 \times 10^8$ raw reads.

Identification of vector integration sites

Vector integration sites (IS) were identified using VISPA2 pipeline³ applied to SLiM-PCR–amplified libraries sequenced with MGI paired-end technology. For each

sequencing library, raw paired-end reads underwent quality control filtering, barcode recognition for sample demultiplexing, and removal of vector sequences. The remaining genomic sequences were aligned to the human reference genome (GRCh37/hg19, February 2019 release).

To quantify the number of genomes corresponding to each clone, we employed the SonicLength approach⁴, which quantifies distinct fragments associated with each IS. This ensured accurate evaluation of clonal abundance within each sample. The final IS dataset included only precisely mapped loci, annotated with the nearest RefSeq gene. Downstream analysis was performed using a new ISAnalytics R package⁵, which integrates VISPA2 output files and supports quality controls, clonal tracking, and inter-sample IS comparison. The full code and documentation are available on GitHub (<https://github.com/calabrialab/ISAnalytics>). To solve “collisions” (identical IS detected across different independent samples), we followed an established method (21), assigning the IS to a single sample based on (i) order of detection or (ii) a ≥ 10 -fold higher abundance in one sample versus the other.

Quality control of the sequencing pools involved: (i) exclusion of samples with raw read counts that were three times lower of the pool’s average, and (ii) removal of suspected cross-sample contamination due to IS collisions, as previously described⁶.

Common insertion site (CIS) analysis was conducted using the Grubbs outlier test⁷ implemented in ISAnalytics. For each patient, the targeting frequency of genes (based on IS within the gene body or ± 100 kb) was normalized to the gene length and log2 transformed. Genes with significantly enriched integration frequency were identified as CIS hits.

Clonal population diversity

An ecological system is maintained stable if the populating species are in equilibrium, suggesting a healthy environment. Analogously, clonal diversity in gene therapy settings can be used as a proxy for hematopoietic health. One commonly used quantitative metric for this is the Shannon diversity index (H-index), which captures both clonal richness (number of distinct clones, or integration sites—IS) and evenness (relative abundance of each clone). H-index is defined as in Equation S1.

This ecological framework has been widely applied to track heterogeneity and complexity of vector-marked cells over time, across tissues, and within differentiated lineages. In this context, ISs are treated as species and their relative abundances reflect clonal prevalence. Sustained high H-index values indicate stable and diverse hematopoiesis, while a sharp decline may signal clonal skewing or potential malignant transformation. In this study, the Shannon diversity index was calculated using the vegan R package and implemented within the ISAnalytics framework to quantify clonal complexity in both in vitro and in vivo settings.

$$H' = - \sum_{i=1}^R p_i \ln p_i$$

Equation S1. Formula for calculating the H-index quantifying clonal complexity, where i denotes a clone (integration site, IS), p_i is the clonal abundance, and R is the total number of clones.

SUPPLEMENTAL FIGURES

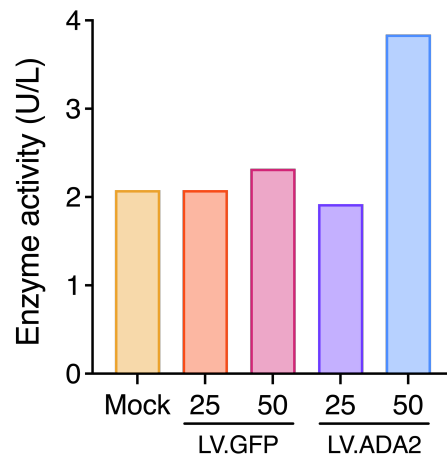


Figure S1. Increased ADA2 activity upon transduction with LV.ADA2 at MOI 50. ADA2 enzymatic activity measured in cell-free supernatants from mPB CD34⁺ cells either mock-transduced or transduced with LV.ADA2 or LV.GFP (control vector) at two multiplicities of infection (MOI 25 and 50).

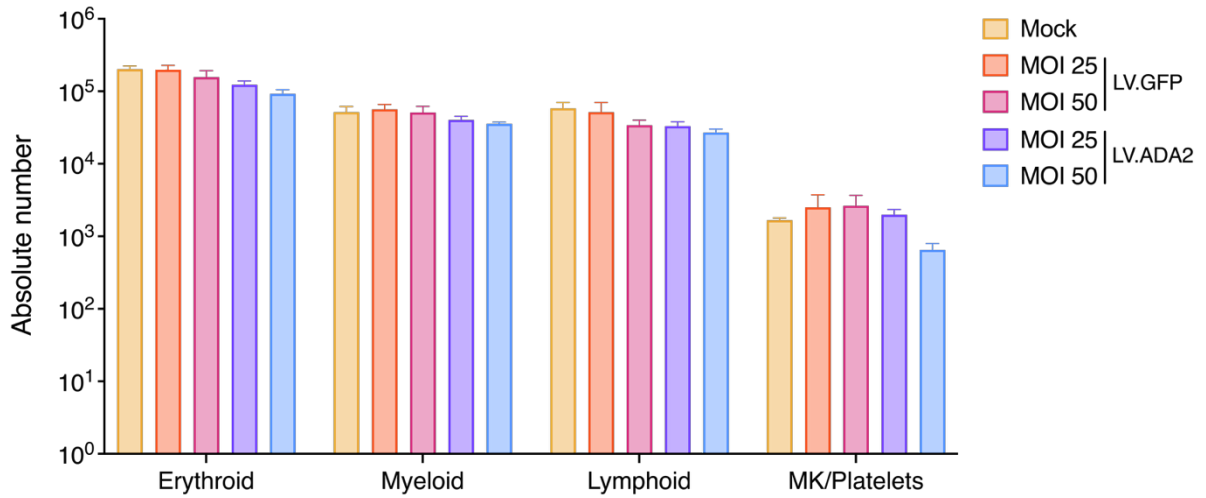


Figure S2. LV-mediated ADA2 overexpression supports normal in vitro differentiation of mPB CD34⁺ cells. In vitro multi-lineage differentiation assay of mPB CD34⁺ cells either mock-transduced or transduced with LV.ADA2 or LV.GFP (control vector) at two multiplicities of infection (MOI 25 and 50). Data are presented as mean±standard error of the mean (SEM).

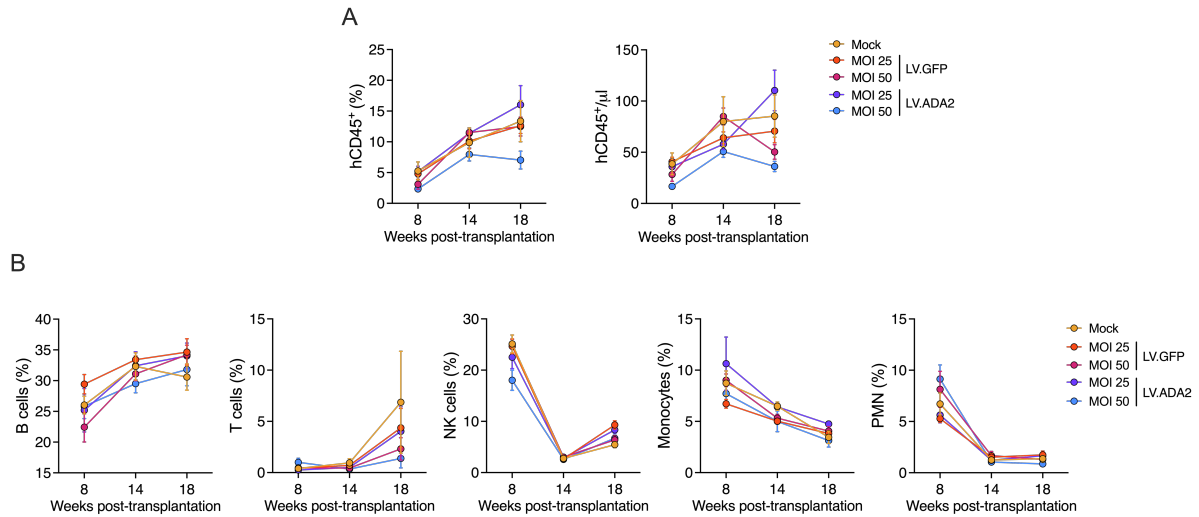


Figure S3. Normal multilineage differentiation of ADA2-transduced mPB CD34⁺ cells from healthy donors in NSGW41 mice. (A) Longitudinal analysis of human chimerism shown as both percentage and absolute number of human CD45⁺ cells in peripheral blood at 8, 14, and 18 weeks post-transplantation (n=5 mice per group). **(B)** Longitudinal analysis of peripheral blood immune subsets—B cells, T cells, NK cells, monocytes, and polymorphonuclear (PMN) cells—at 8, 14, and 18 weeks post-transplantation (n=5 mice per group).

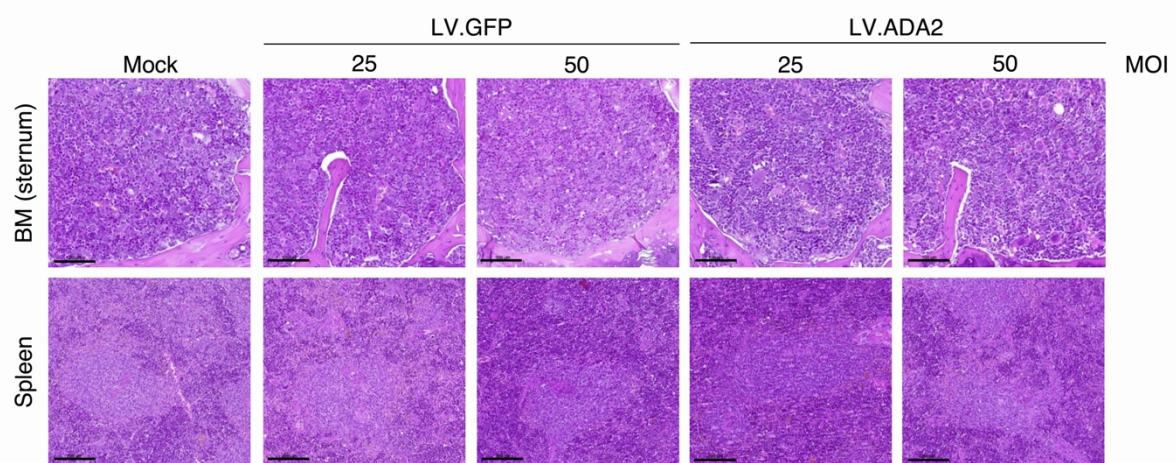


Figure S4. No evidence of in vivo toxicity associated with LV-mediated ADA2 overexpression. Hematoxylin and eosin (H&E) staining of representative sections from the sternum BM and spleen of NSGW41 mice transplanted with mPB CD34⁺ cells from healthy donors (HDs), either mock-transduced or transduced with LV.ADA2 or LV.GFP at a multiplicity of infection (MOI) of 25 or 50. Scale bars: 100 μ m in bone marrow (sternum), 200 μ m in spleen.

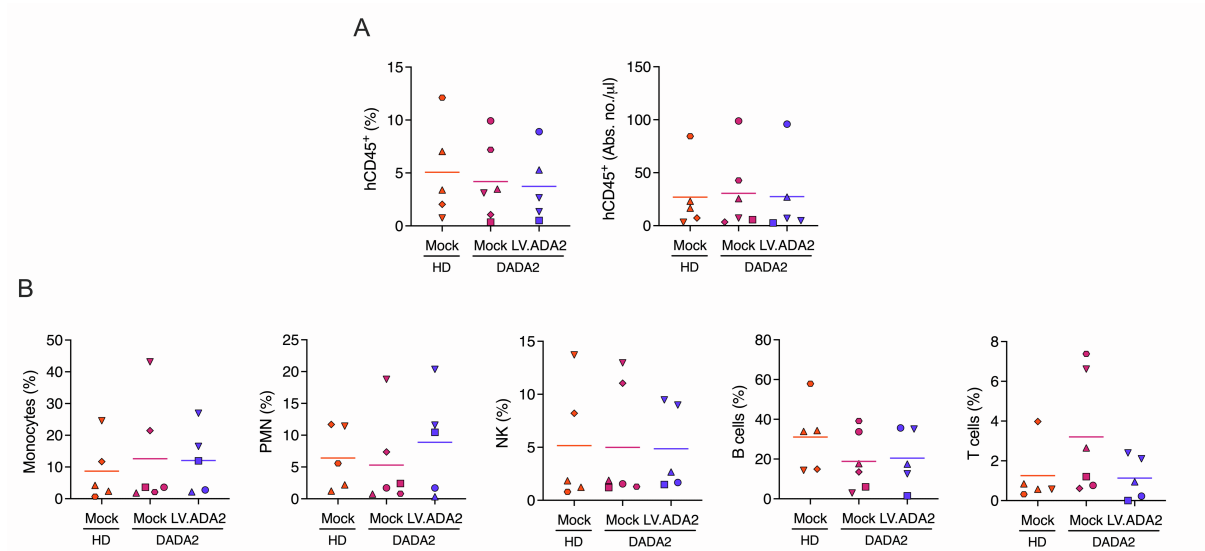


Figure S5. LV.ADA2 gene therapy supports multilineage hematopoietic differentiation of ADA2-transduced patient-derived HSPCs in NSGW41 mice. (A) Human chimerism in peripheral blood was assessed at 20 weeks post-transplantation and is shown as both percentage and absolute number of human CD45⁺ cells per µl. **(B)** Percentages of mature immune cell populations—monocytes, polymorphonuclear cells (PMNs), B cells, T cells, and NK cells—were quantified within the human CD45⁺ compartment of peripheral blood at the same time point. Data include recipients of mock-transduced healthy donor cells, mock-transduced DADA2 cells, and LV.ADA2-transduced DADA2 cells. Bars denote mean.

SUPPLEMENTAL TABLES

Table S1. Number and distribution of unique integration sites in all in vitro and in vivo datasets.

Table S2. Sample characteristics and number of integration sites retrieved

Donor	Cell source	Vector and dose	Tissue	VCN_avg	DNA (ng)	nIS
HD-A	mPB HD CD34+	LV.ADA2 MOI 25	Post-LC	0.40	10.58	346
HD-A	mPB HD CD34+	LV.ADA2 MOI 50	Post-LC	3.40	10.66	2984
HD-A	mPB HD CD34+	LV.GFP MOI 25	Post-LC	0.21	10.66	158
HD-A	mPB HD CD34+	LV.GFP MOI 50	Post-LC	0.89	10.61	712
HD-A	mPB HD CD34+	LV.ADA2 MOI 25	Mouse total BM	0.41	10.45	445
HD-A	mPB HD CD34+	LV.ADA2 MOI 50	Mouse total BM	3.72	10.53	1796
HD-A	mPB HD CD34+	LV.GFP MOI 25	Mouse total BM	0.18	10.52	161
HD-A	mPB HD CD34+	LV.GFP MOI 50	Mouse total BM	0.81	10.45	725
HD1	HD BM CD34+	LV.ADA2 MOI 50	Post-LC	7.00	10.53	2615
HD2	HD BM CD34+	LV.ADA2 MOI 50	Post-LC	15.90	10.46	7661
HD3	HD BM CD34+	LV.ADA2 MOI 50	Post-LC	0.67	10.54	459
HD4	HD BM CD34+	LV.ADA2 MOI 50	Post-LC	0.95	10.37	576
Pt1	DADA2 BM CD34+	LV.ADA2 MOI 50	Post-LC	3.95	10.49	1303
Pt2	DADA2 BM CD34+	LV.ADA2 MOI 50	Post-LC	10.78	10.44	5395
Pt3	DADA2 BM CD34+	LV.ADA2 MOI 50	Post-LC	6.18	10.40	5521
Pt4	DADA2 BM CD34+	LV.ADA2 MOI 50	Post-LC	16.13	10.40	4470
Pt5	DADA2 BM CD34+	LV.ADA2 MOI 50	Post-LC	8.14	10.61	2808
Pt6	DADA2 BM CD34+	LV.ADA2 MOI 50	Post-LC	1.26	10.55	782
HD1	HD BM CD34+	LV.ADA2 MOI 50	Mouse total BM	5.77	10.57	168
HD2	HD BM CD34+	LV.ADA2 MOI 50	Mouse total BM	11.55	10.35	303
HD3	HD BM CD34+	LV.ADA2 MOI 50	Mouse total BM	0.72	10.61	101
HD4	HD BM CD34+	LV.ADA2 MOI 50	Mouse total BM	0.42	10.51	15
Pt1	DADA2 BM CD34+	LV.ADA2 MOI 50	Mouse total BM	3.54	10.40	103
Pt4	DADA2 BM CD34+	LV.ADA2 MOI 50	Mouse total BM	12.80	10.61	47
Pt5	DADA2 BM CD34+	LV.ADA2 MOI 50	Mouse total BM	2.01	10.53	133
Pt6	DADA2 BM CD34+	LV.ADA2 MOI 50	Mouse total BM	0.50	10.40	105

Healthy donors (HD) or DADA2 patients (Pt) (Donor column) were used as source of mobilized peripheral blood (mPB) or bone marrow (BM) derived CD34+ cells (column cell source) and transduced with LV.ADA2 or LV.GFP at a MOI of 25 or 50 (column Vector and Dose). Integrations were retrieved from cells after 14-day in vitro liquid culture (Post-LC) or BM cells from NSGW41 recipient mice at 20 weeks post-transplantation (column Tissue). The table reports the average vector copy number (VCN), the amount of genomic DNA used for SLiM-PCR, and the number of unique integration sites (nIS) identified per condition are indicated.

References

1. Cesana, D., Calabria, A., Rudilosso, L., Gallina, P., Benedicenti, F., Spinozzi, G., Schioli, G., Magnani, A., Acquati, S., Fumagalli, F., et al. (2021). Retrieval of vector integration sites from cell-free DNA. *Nat Med* 27, 1458-1470. 10.1038/s41591-021-01389-4.
2. Firouzi, S., Lopez, Y., Suzuki, Y., Nakai, K., Sugano, S., Yamochi, T., and Watanabe, T. (2014). Development and validation of a new high-throughput method to investigate the clonality of HTLV-1-infected cells based on provirus integration sites. *Genome Med* 6, 46. 10.1186/gm568.
3. Spinozzi, G., Calabria, A., Brasca, S., Beretta, S., Merelli, I., Milanesi, L., and Montini, E. (2017). VISPA2: a scalable pipeline for high-throughput identification and annotation of vector integration sites. *BMC Bioinformatics* 18, 520. 10.1186/s12859-017-1937-9.
4. Berry, C.C., Gillet, N.A., Melamed, A., Gormley, N., Bangham, C.R., and Bushman, F.D. (2012). Estimating abundances of retroviral insertion sites from DNA fragment length data. *Bioinformatics* 28, 755-762. 10.1093/bioinformatics/bts004.
5. Pais, G., Spinozzi, G., Cesana, D., Benedicenti, F., Albertini, A., Bernardo, M.E., Gentner, B., Montini, E., and Calabria, A. (2023). ISAnalytics enables longitudinal and high-throughput clonal tracking studies in hematopoietic stem cell gene therapy applications. *Brief Bioinform* 24. 10.1093/bib/bbac551.
6. Biffi, A., Montini, E., Lorioli, L., Cesani, M., Fumagalli, F., Plati, T., Baldoli, C., Martino, S., Calabria, A., Canale, S., et al. (2013). Lentiviral hematopoietic stem cell gene therapy benefits metachromatic leukodystrophy. *Science* 341, 1233158. 10.1126/science.1233158.

7. Biffi, A., Bartolomae, C.C., Cesana, D., Cartier, N., Aubourg, P., Ranzani, M., Cesani, M., Benedicenti, F., Plati, T., Rubagotti, E., et al. (2011). Lentiviral vector common integration sites in preclinical models and a clinical trial reflect a benign integration bias and not oncogenic selection. *Blood* 117, 5332-5339. 10.1182/blood-2010-09-306761.